

# Collapse-Stretching Transition for Polymer Brushes. Preferential Solvation

P. Auroy\* and L. Auvray

Laboratoire Léon Brillouin, CEA-CNRS, CEN Saclay, 91191 Gif Sur Yvette Cedex, France

Received December 20, 1991; Revised Manuscript Received April 20, 1992

**ABSTRACT:** We have investigated by small-angle neutron scattering techniques the collapse-stretching transition of grafted poly(dimethylsiloxane) chains. Two ways have been used for inducing this transition: modifying the chemical composition in a binary mixture or changing the temperature in a given solvent around the  $\theta$  point. The first method reveals a spectacular preferential solvation effect, provided that the grafting density is high enough. The second method is more graduate: the thickness of the interface is a linear function of temperature in the range we have investigated.

## Introduction

For several years, we have been studying the polymers at the solid-liquid interface. We have mainly focused our attention to the conformation of the chains in a given solvent, either when they are adsorbed<sup>1</sup> or grafted<sup>2</sup> onto a solid substrate. Two types of solvent have been used: poor solvents in which the chains are always collapsed and good solvents that under certain circumstances can induce a strong stretching of the polymers. The structure of the interface is also affected by the type of the solvent. In the case of grafted chains, in the brush regime (where the polymers are densely grafted), the interface in the presence of a poor solvent is dense and of well-defined thickness, while a good solvent induces a strong stretching of the polymers and a smoother shape of the interfacial profile with large concentration fluctuations. What happens between these two well-characterized situations?

We have tried to answer to this question. We have restricted our study to grafted layers, because this system is the best controlled and the two extreme states (collapse versus stretching) are very well described. Two different ways have been used to vary continuously the solvent quality: either, in a given solvent, changing the temperature or mixing in different proportions of a poor and a good solvent. The first method allows us to seek quite properly whether there are some critical phenomena like a coil-globule transition<sup>3,4</sup> driven by the temperature of the solvent. The second method tackles a more complicated problem owing to the possibility of preferential solvation.

This latter question has been paid some attention in the past, in particular because it is of great importance for industrial applications. But only very few theoretical papers deal with this problem and either from a very specific point of view<sup>5</sup> or with only partial conclusions<sup>6</sup> due to computational limitations. The experimental studies<sup>7</sup> of the preferential solvation are much more numerous but their conclusions are very scattered and sometimes opposite. Furthermore, they have only focused on the thermodynamics of dilute polymer solutions in a binary mixture of solvents. These experiments are non-local; i.e. they measure the size of the coils (more or less directly) without knowing precisely the local volume fraction of each solvent inside or just around the coil. In these experiments, the measurement of the size of the coils and the estimation of the amount of preferred solvent are strongly correlated. Furthermore, they are intrinsically limited by the eventual demixtion of the solution and therefore one cannot really explore the collapse region.

All these restrictions are avoided in our study because the chains are attached (grafted) and confined in an interface. Even in a poor solvent, using small-angle neutron scattering (SANS) techniques, it is possible to characterize the average concentration profile (in particular, the thickness of the layer). Moreover, by varying the neutron refractive index of the solvent mixture, we are able to determine the local composition of the solvent trapped inside the polymer interface.

In the first section of this paper, we describe in more detail the experimental system and recall a few technical points about the SANS techniques. In section II, we present and discuss the results concerning the collapse-stretching transition in a binary mixture. In particular, we emphasize the effects of preferential solvation. Then we study briefly the influence of the grafting density on this transition (section III). In the last part, the collapse-stretching transition is induced by the temperature. We shall compare the results in this case with those obtained with the binary mixtures.

## I. Experimental Section

**I.1. System.** Throughout this paper, only two samples are examined. They are identical except for their grafting density. Their main features are shown in Table I. They have been prepared by grafting long, monodisperse poly(dimethylsiloxane) (PDMS) chains ( $M_w = 166\,500$ , polydispersity index 1.10) onto a porous silica, as previously described.<sup>2</sup> The silica surface has been modified before the grafting reaction in order to prevent the natural adsorption of PDMS. It has been partially esterified with stearyl alcohol.<sup>8</sup> The grafting density has been adjusted by using two different concentrations of free polymer in the reaction bath.

Three solvents and their corresponding perdeuterated species have been used: methanol and dichloromethane which are respectively a poor and a good solvent for PDMS at room temperature and styrene which is a  $\theta$  solvent for PDMS at 29.7 °C for [H]styrene and 34.95 °C for [D]styrene.<sup>9</sup> Though this slight difference, we assume that for all the solvents in this article, the ordinary and the deuterated species are thermodynamically equivalent. In particular, we assume that they have the same interaction with the polymer. All these solvents are of high purity grade. They have always been mixed in order to match the scattering length density of the silica (i.e.  $3.484 \times 10^{10} \text{ cm}^{-2}$ ). This point will be further developed in the next section. We call  $x_D$  the volume fraction of the perdeuterated solvent compared to the total volume of the same solvent (H or D).

**I.2. SANS Techniques and Data Treatment.** We assume in this paragraph that the scattering experiments are done under the contrast matching condition with only one solvent. Therefore the scattering intensity  $I(q)$  is only due to the polymer interface ( $q$  is the momentum transfer).<sup>10</sup> Our method gives a great importance to the analysis of the data in the reciprocal space (as

**Table I**  
Main Characteristics of the Two Samples of This Paper

	$\gamma$ (mg/m <sup>2</sup> )	$D^a$ (Å)	thickness in methanol (Å)	thickness in dichloromethane (Å)
sample 1	19.7	37	212	815
sample 2	2.7	100	59	223

<sup>a</sup>  $D$  is the average distance between grafting points.

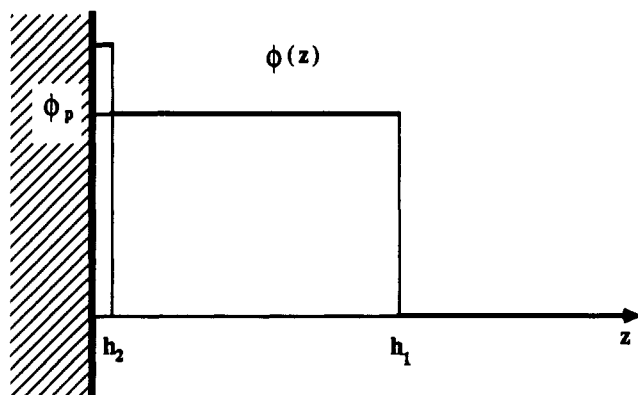


**Figure 1.** Schematic shape of the interfacial concentration profile. The narrow step of extension  $h_2$  corresponds to the thin layer of stearyl alcohol.

they were obtained). For determining the thickness of the layer, we use the plot  $q^2 I(q)$  vs  $q^2$ . If we assume that the interfacial density profile  $\phi(z)$  is a step (of height  $h$ ,  $z$  is the coordinate normal to the surface), then, under contrast matching conditions, it can be shown that

$$q^2 I(q) = 2\pi(S/V)\Delta_0^2 \gamma^2 \left(1 - \frac{q^2 h^2}{12}\right) \quad (1)$$

provided that

$$qh \ll 1 \quad (2)$$

$\Delta_0 = n_p - n_s$  is the difference between the scattering length density of the polymer ( $n_p$ ) and that of the solvent ( $n_s$ ) which is equal to that of the silica.  $S/V$  is the specific surface area of the substrate (2.5 m<sup>2</sup>/cm<sup>3</sup>) and  $\gamma = \int_0^\infty \phi(z) dz$  is the amount of polymer per unit area.

For the samples of this article, we cannot neglect the contribution of the stearyl alcohol layer. If we assume that the density profile can be roughly decomposed in two steps (cf. Figure 1), then the same plot as above can be used to determine the thickness of the polymer layer but instead of (1), one has

$$q^2 I(q) = 2\pi(S/V)\Delta_0^2 (\gamma_1 + \gamma_2)^2 \left(1 - \frac{\alpha q^2 h_1^2}{12}\right) \quad (3)$$

$$\alpha = \frac{\gamma_1^2 + 4\gamma_1\gamma_2}{(\gamma_1 + \gamma_2)^2}$$

where the indexes 1 and 2 refer respectively to the polymer and to the stearyl chains. Equation 3 is valid only if  $\gamma_2 h_2 \ll \gamma_1 h_1$ , which is the case for both samples of this article since the stearyl layer is very thin.

In Figure 2, we have reported the scattering intensity for the "bare" sample, i.e. the esterified silica immersed in dichloromethane (●). Equation 1 allows one to determine  $\gamma_2 = 10.1$  Å.  $h_2$  is not measurable (the spectrum is flat). But, anyway, its value is less than 10 Å. It should be noticed here that this sample is not the esterified silica just before the polymer grafting (spectrum □) but it has been submitted to a subsequent thermal treatment for 24 h (with the same conditions of temperature, pressure, and solvent as for the grafting of PDMS). We have indeed observed that the grafted stearyl chains are partially removed by such treatment. This is clearly visible with Figure 3, where we have reported the amount of grafted stearyl alcohol as a function of duration of the thermal treatment.

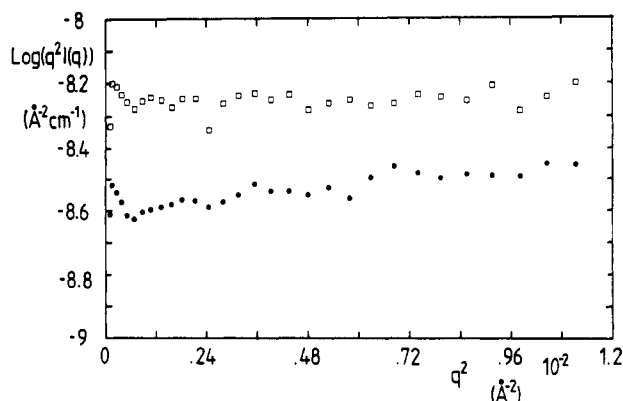


**Figure 2.** Scattering intensity of the "bare" (without polymer) substrate before (□) and after (●) a thermal treatment of 24 h (plot of  $q^2 I(q)$  vs  $q^2$ ). The extrapolated value at low  $q$  allows us to determine the amount of grafted stearyl alcohol (see eq 1).

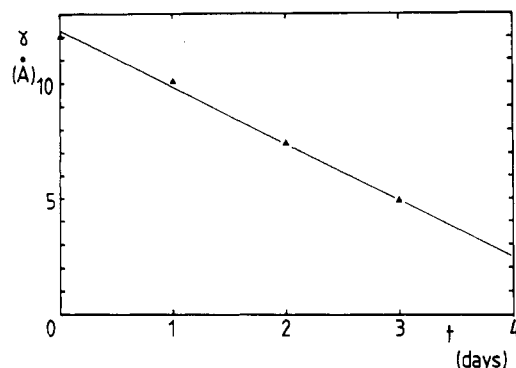


**Figure 3.** Plot of the amount of grafted stearyl alcohol per unit area  $\gamma$  (in Å) as a function of duration of the thermal treatment  $t$  (in days).

We also use very often a second type of plot,  $q^4 I(q)$  versus  $q$ , that allows us to emphasize the singularities (like a discontinuity or a steep decrease) of the interfacial concentration profile. For a step (of height  $h$ )

$$q^4 I(q) = 4\pi(S/V)\Delta_0^2 (1 - \cos qh) \phi_p^2 \quad (4)$$

$\phi_p$  is the polymer concentration inside the step. This plot does not require one to take care about the thin layer of stearyl alcohol because the corrections which it could introduce are of the order of  $q^2 h_2^2 \ll 1$  in the whole experimental  $q$  range.

Finally, if there are some concentration fluctuations of the Orstein-Zernike type, the scattering intensity follows a Lorentzian-type law and the best plot for revealing such behavior is the inverse of the scattering intensity  $I(q)^{-1}$  versus  $q^2$ .

$$I(q)^{-1} \approx 1 + q^2 \xi^2 \quad (5)$$

where  $\xi$  is the typical correlation length of the concentration fluctuations.

Therefore, these three behaviors appear in different  $q$  ranges, depending on the  $qh$  values. For the samples of grafted polymer, the very small angle domain,  $q < 10^{-2}$  Å<sup>-1</sup> (eq 3) concerns only a few of the first points of the spectra (for instance, only the first five points for Figure 7a); the intermediate  $q$  range,  $10^{-2} < q < 5 \times 10^{-2}$  Å<sup>-1</sup>, reveals the typical behavior described by eq 4, and finally, the "high  $q$  domain" ( $q > 5 \times 10^{-2}$  Å<sup>-1</sup>) is eventually dominated by the concentration fluctuations (eq 5).

**I.3. Contrast Variation around the Scattering Length Density of the Silica.** All the experiments described below have been done under the contrast matching condition: that means that the solvent has the same scattering length density as the silica. If we use only one solvent (pure methanol, pure dichloromethane, or pure styrene), this condition imposes a unique isotopic mixture for this given solvent. We call  $x_D$  the volume fraction of the perdeuterated component. The matching of the silica is achieved when  $x_D = 62.2\%$  for methanol,  $x_D = 90\%$  for dichloromethane, and  $x_D = 52.7\%$  for styrene).<sup>11</sup>

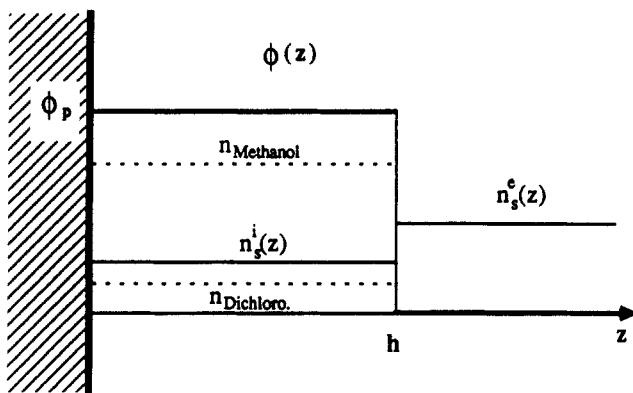


**Figure 4.** Assumed scattering length density profiles for the solvent. The polymer concentration profile has also been drawn. This picture corresponds to a strong preferential solvation of dichloromethane, in a 50/50 binary mixture.  $n_s^i$  and  $n_s^e$  refer respectively to the solvent inside (outside) the interface. Dotted lines refer to the scattering length density of methanol and dichloromethane. In bulk, these two solvents form a mixture that has the same scattering length density as that of the silica (contrast matching in average).

If two solvents are used (in a given ratio), many compositions are possible for achieving the matching condition. When each component of the binary mixture matches the silica (we call this situation "perfect" matching), it is not possible to detect a preferential solvation because each solvent has the same scattering length density (equal to that of the silica). In that case, the scattering comes only from the polymer (eq 4). But if the contrast matching is achieved only in average (each component being withdrawn from the average imposed by the silica), then it is possible to determine the precise chemical composition of the solvent inside the layer. Indeed, let us assume that the solvent density profile, for each component of the binary mixture, is allowed to be modified by the preferential adsorption only within the polymer interface and that these solvent density profiles can be modeled by a step of height  $h$  (the same as for the polymer layer) (Figure 4). Under these conditions, it can be shown that eq 4 becomes

$$q^4 I(q) = 4\pi(S/V)(\Delta\phi_p + \delta)^2(1 - \cos qh) \quad (6)$$

$\Delta = n_p - n_s^i$  and  $\delta = n_s^i - n_s^e$  are respectively the difference between the neutron refractive index of the polymer  $n_p$  (the solvent inside the layer,  $n_s^i$ ) and that of the solvent inside the layer  $n_s^i$  (outside,  $n_s^e$ ). Equations 1 and 3 are also modified in the same way. Equation 6 tells us that, if there is some preferential adsorption, it will be revealed by comparison with the experiment done at perfect matching. The spectrum  $q^4 I(q)$  vs  $q$  will keep the same shape (oscillations), but the contrast (the amplitude of the oscillations) will be affected by the shift in the chemical composition of the solvent inside the layer.

## II. Collapse-Stretching Transition in a Binary Mixture at High Grafting Density

In this part, we focus on the sample at high grafting density (sample 1) immersed in different mixtures of methanol and dichloromethane. We call  $G$  the average volume fraction of dichloromethane in the mixture ( $G = 1$ , pure dichloromethane;  $G = 0$ , pure methanol).

**II.1. Variation of the Thickness of the Interface as a Function of  $G$ .** We have reported in Figure 5 the values of the thickness  $h$  of the grafted layer versus  $G$ . All these data have been obtained under the perfect matching condition, using the  $q^2 I(q)$  vs  $q^2$  plot (with an adequate  $q$  range) and assuming that the density profile is a step. This is obviously a crude approximation especially for the data obtained at  $G$  close to 1. We shall discuss this point in more detail in a subsequent section. But it should be noticed here that the shape of the curve of Figure 5 would not be very different from the exact  $h(G)$  curve anyway.

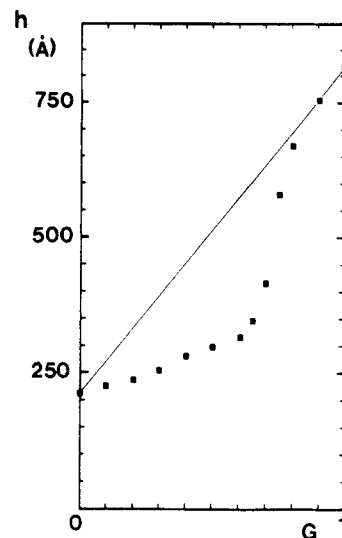


**Figure 5.** Thickness of the polymer interface (sample 1) as a function of the chemical composition  $G$  of the binary mixture methanol-dichloromethane.

Figure 5 shows that the interface goes from a "collapsed" state to an expanded state in a very narrow (15%) range of variation of  $G$ . As  $G$  increases from 0 to 1, the interface reacts as if it would remain collapsed. In this sense, the transition can be called "retarded".

**II.2. Preferential Solvation.** Obviously, it was very important to seek whether or not this effect is related to a preferential solvation. For that purpose, we have done the experiment described above. We have compared the spectra obtained in a 50/50 mixture of methanol and dichloromethane ( $G = 0.5$ ) but with two different balances in the isotopic composition. The mixture  $G = 0.5$  has been chosen because of the shape of the curve  $h(G)$ . At  $G = 0.5$ , this curve is the most out of line and, therefore, a possible preferential solvation would be maximum at this point. The two mixtures we have used consisted of equal volumes of methanol ( $x_D = 62.2\%$ ) and dichloromethane ( $x_D = 90\%$ ) (mixture 1) and equal volumes of methanol ( $x_D = 90.6\%$ ) and dichloromethane ( $x_D = 0\%$ ) (mixture 2). Both mixtures ensure the matching of the silica, but the first one does it for each component (perfect matching) while the second one only in average.

We have reported in Figure 6a the scattering intensity of the bare silica immersed in these two mixtures and also in pure methanol and in pure dichloromethane. Figure 6b shows the spectra obtained for the same samples but with a different  $q$  range. It is clear that there are no peculiar effects with these mixtures. We could only interpret the slight difference between the two binary mixtures as a result of a thin layer of adsorbed methanol. But this effect, whatever it comes from, is very weak, detectable only at high  $q$ . One can consider both mixtures as roughly equivalent for the bare silica.

In Figure 7, we have reported the spectra of the intensity scattered by the dense grafted layer in mixtures 1 and 2 (with two different  $q$  ranges; neutron wavelengths (a)  $\lambda = 15$  Å, (b)  $\lambda = 6.48$  Å). Both spectra have rigorously the same shape<sup>12</sup> (this is especially striking at low  $q$ ), but the contrast is much enhanced with mixture 2. This is the signature of a preferential solvation.

Which solvent has the greatest affinity for the PDMS interface? It is necessary to return to the basic eqs 4 and 6. We call  $\beta_1^2(\beta_2^2)$  the maximum value of  $q^4 I(q)$  in mixture

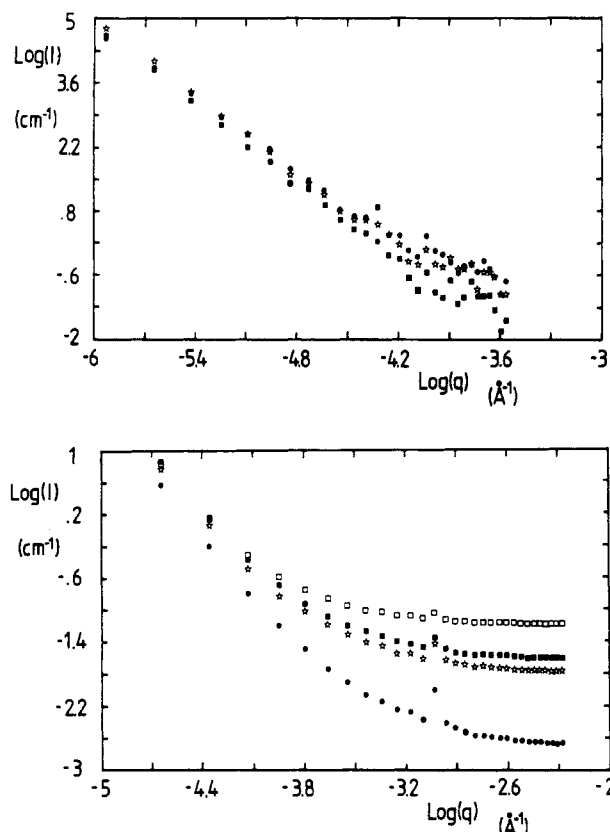


**Figure 6.** Comparison of the scattering intensity for the bare substrate with different mixtures: (●) pure dichloromethane, (☆) mixture 1; (■) mixture 2; (□) pure methanol. Neutron wavelengths: (a, top)  $\lambda = 15$  Å; (b, bottom)  $\lambda = 6.48$  Å.

1 (mixture 2). We must have

$$\frac{|\Delta_0 \phi_p|}{\beta_1} = \frac{|\Delta \phi_p + \delta|}{\beta_2}$$

or

$$\Delta \phi_p + \delta = \pm \tau$$

with

$$\tau = \frac{\beta_2}{\beta_1} |\Delta_0 \phi_p|$$

From the value of  $\beta_1$ , one can calculate  $\phi_p$ . We have found  $\phi_p = 0.64$ .<sup>13</sup> We call now  $n_p$  the scattering length density of the polymer and  $n_s^i$  ( $n_s^e$ ) the scattering length density of the solvent inside (outside) the interface. Then

$$(n_p - n_s^i) \phi_p + (n_s^i - n_s^e) = \pm \tau$$

or

$$n_s^i = \frac{\pm \tau + n_s^e - n_p \phi_p}{1 - \phi_p}$$

Taking  $n_s^e = 3.484 \times 10^{10} \text{ cm}^{-2}$ , one gets only one possibility for  $n_s^i$  (the other having no sense):

$$n_s^i = 1.861 \times 10^{10} \text{ cm}^{-2} \quad (\text{from the data obtained with } \lambda = 15 \text{ Å})$$

$$n_s^i = 2.178 \times 10^{10} \text{ cm}^{-2} \quad (\text{from the data obtained with } \lambda = 6.48 \text{ Å})$$

Therefore, the solvent that has the greatest affinity for the PDMS interface and solvates it preferentially is the

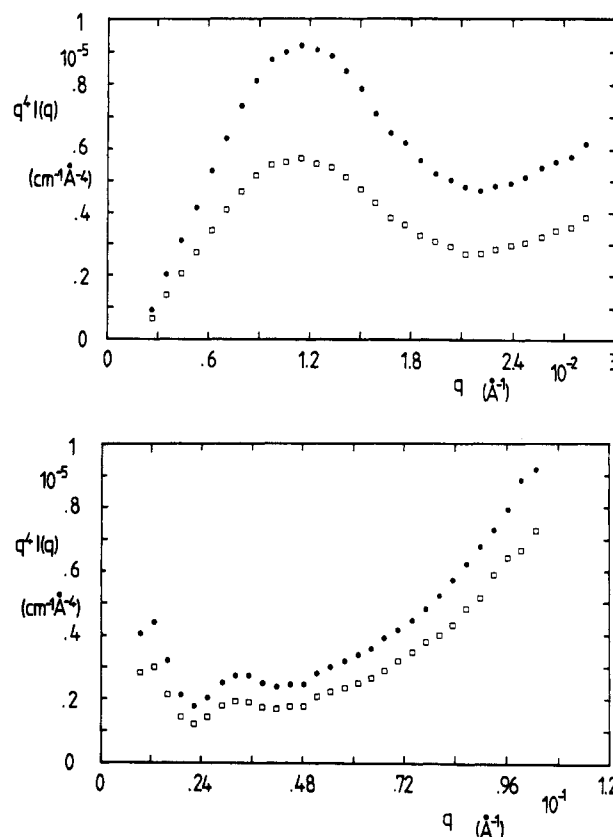


**Figure 7.** Comparison of the scattering intensity at  $G = 0.5$  for two different isotopic balances (plot of  $q^4 I(q)$  vs  $q$ ): (□) mixture 1; (●) mixture 2. Neutron wavelengths: (a, top)  $\lambda = 15$  Å; (b, bottom)  $\lambda = 6.48$  Å.

dichloromethane. One can estimate that the solvent confined in the interface is composed of 96% of dichloromethane (87% using the data obtained with  $\lambda = 6.48$  Å). It is therefore almost pure dichloromethane, while the bath keeps its 50/50 composition.

Returning to a somewhat technical point, one can discuss the validity of the main assumptions hidden in our determination of the chemical composition of the solvent trapped in the brush. It is based on the fact that the interfacial density profile of this solvent is also a step of height  $h$  (the same as for the polymer) (see Figure 4). Consequently, the spectra that have been obtained with different contrasts are exactly proportional (cf. eqs 4 and 6). As we have seen in Figure 7, this is roughly verified with mixtures 1 and 2. Hence, our assumptions seem to be valid. However, a careful examination of the data leads to the conclusion that the ratio  $\beta_2/\beta_1$  slightly increases with  $q$ . This can be interpreted at least in two different ways: there could be some multiple scattering, or the dichloromethane solvates the interface more strongly close to the wall than near the outer edge of the interface. The first explanation is very little likely, especially for the spectra obtained with the wavelength of 6.48 Å. The second interpretation is more satisfactory, in particular because the density profile of the polymer itself is not a perfect step but something that decreases to zero in a more gradual way. In the next section, we shall see that the preferential solvation effect is much less pronounced when the grafting density is smaller. This suggests that the strength of this effect should be related to the local concentration  $\phi(z)$  and therefore, close to the wall, the solvent would be pure dichloromethane, whereas around the outer edge of the interface, it would reach its bulk composition gradually. This  $z$  dependence of the preferential solvation leads to an increase of the ratio  $\beta_2/\beta_1$

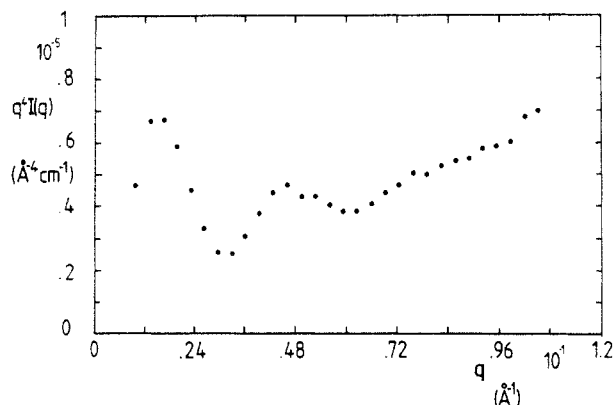


**Figure 8.** Scattering intensity of the polymer interface (sample 1) immersed in the mixture  $G = 0.1$  (plot of  $q^4 I(q)$  vs  $q$ ).

with  $q$ , as we observe. Anyway, this picture, even if reasonable, does not alter deeply our conclusions, and at a zero-order approximation, our assumptions are completely valid.

On the basis of naive arguments, it is not really surprising that the good solvent solvates preferentially the polymer interface. But what is not obvious and somewhat paradoxical is that this effect is associated with a (strong) collapse of the chains. This has been predicted to some extent by Monte-Carlo calculations.<sup>6</sup> Magda et al. have studied the thermodynamics of polymer solutions in binary solvent mixtures. The length of the chains was quite short and quantitative information has been obtained only with equimolar mixed solvent in the limit of infinite dilutions. Therefore, this study, though the closest, is not directly applicable to our work. But it is nevertheless interesting to compare qualitatively the results. The main conclusion of Magda et al. is that the chains contract themselves compared to the "equivalent" pure single component, through the preferential solvation of the good solvent. The contraction takes place in order to diminish this preferential solvation. And the monomer-monomer correlations differ considerably from the pure solvent case: they tend to promote the configurations for which the preferred solvent binds the polymer at more than one site. We believe that these arguments apply qualitatively to our experimental study. Nevertheless, the effects we have observed are much more pronounced than those described in the literature.<sup>14</sup>

**II.3. Shape of the Interfacial Concentration Profile.** We have not systematically tried to determine the shape of the interfacial concentration profile. This would have required a complete study including contrast variation experiments which consume much beam time.

Nevertheless, two important features are clear: before the transition ( $G \leq 0.6$ ), the density profile is steplike, without any concentration fluctuations. As we have seen previously (Figure 6), for  $G = 0.5$ , the scattering law agrees well with eq 4. This is a fortiori true for  $G < 0.5$ . (See Figure 8 which corresponds to  $G = 0.1$ .) In Figure 9, we have reported the ratio  $\zeta = \phi_s/(\gamma/h)$  as a function of  $G$ . These data have been obtained under the perfect matching condition;  $h$  and  $\phi_s$  have been worked out using the step model (eqs 3 and 4). Notice that  $\gamma$  is determined independently of any model. The ratio  $\zeta$  is constant, nearly equal to 1 for  $G \leq 0.6$ ; that is again consistent with the assumed step model. For  $G \geq 0.7$ , this ratio suddenly increases. For  $G > 0.8$ ,  $\zeta$  could not be determined because the Porod plateau vanished. The raise of  $\zeta$  is related to the abrupt variation of  $h$ : the layer expands dramatically.

This sudden change of  $\zeta$  is associated with a great variation of the shape of the scattering intensity at low  $q$

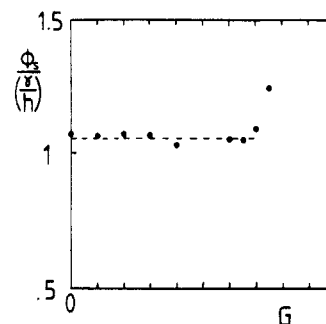


**Figure 9.** Variation of the ratio  $\zeta = \phi_s/(\gamma/h)$  as a function of  $G$ .

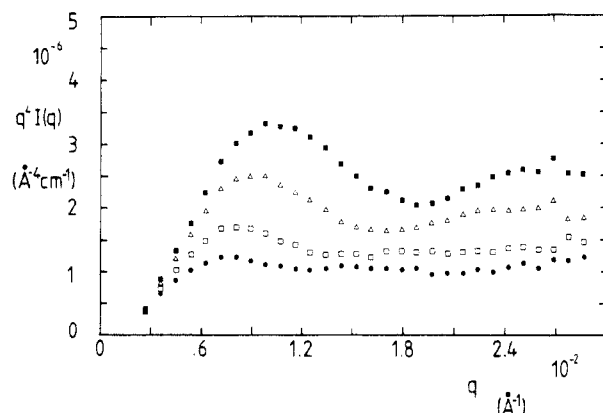


**Figure 10.** Scattering intensity of the polymer interface (sample 1) for  $G = 0.6$  (■),  $G = 0.65$  (Δ),  $G = 0.7$  (□),  $G = 0.75$  (●) (plot of  $q^4 I(q)$  vs  $q$ ).

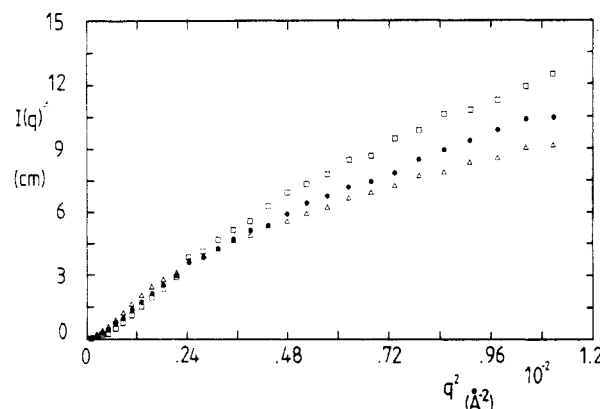


**Figure 11.** Plot of the inverse of the scattering intensity for sample 1 versus  $q^2$ : (□)  $G = 0.65$ ; (●)  $G = 0.75$ ; (Δ)  $G = 0.9$ .

(Figure 10). In a narrow range of  $G$  ( $0.6 \leq G \leq 0.75$ ), the characteristic oscillations disappear as the asymptotic horizontal level of  $q^4 I(q)$  (Porod's plateau) goes down. This can be interpreted by a smoothening of the density profile. But meanwhile, the scattering intensity at higher  $q$  is also dramatically modified. This is due to the grow of concentration fluctuations. In Figure 11, we have plotted the inverse of the scattering intensity as a function of  $q^2$ . These spectra seem to follow eq 5. As we have explained elsewhere,<sup>2b</sup> we should take into account the fact that, under the contrast matching condition, the scattering intensity is the sum of two terms: the first due to the average concentration profile and the second due to the concentration fluctuations. For separating both contributions, one should do a contrast variation experiment. Nevertheless, in the intermediate  $q$  range, the second contribution dominates and therefore one can obtain an estimation of the typical length of the monomer-monomer correlations, ignoring the scattering of the average density profile. The fit of the three spectra of Figure 11 with the

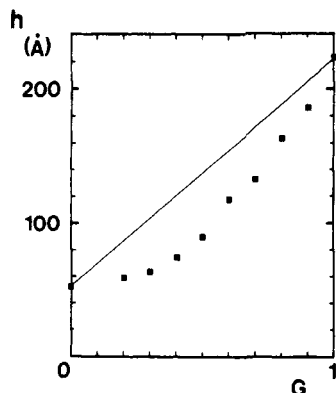


**Figure 12.** Thickness of the polymer interface (sample 2) as a function of the chemical composition  $G$  of the binary mixture methanol-dichloromethane.

Lorentzian law (5) gives the results shown in Figure 15.  $\xi$  is a decreasing function of  $G$ . One recovers here a well-known property of polymer solutions.<sup>15</sup>  $\xi$  varies inversely with the temperature.

The presence of concentration fluctuations that contribute mostly to the scattering intensity makes the precise determination of the average density profile impossible for  $G > 0.6$  with only the contrast matching experiment. Nevertheless, it is clear that this interfacial profile becomes much smoother for  $G > 0.6$ : the polymer-solvent boundary is no longer sharp.

### III. Influence of the Grafting Density on the Collapse-Stretching Transition and on the Preferential Solvation

In this section, we consider the collapse-stretching transition in a binary mixture for sample 2. We have done the same experiments as above, but now the grafting density of the layer is much smaller (see Table I).

**III.1. Variation of  $h$  with  $G$ .** As before, the thickness of the interface is an increasing function of  $G$  (Figure 12). But the variation of  $h$  is never abrupt. The curve is still convex which tends to prove that there is also a preferential solvation. We did not use different isotopic balances which would have given a definitive answer. We believe however that dichloromethane is again responsible for this preferential adsorption. But the effects are much weaker than for the previous sample. This is due to the grafting density that is 7 times smaller. For sample 2, in pure methanol, the chains are not in the brush regime: i.e. the average distance between grafting sites  $D$  ( $D = 100$  Å) is greater than the thickness of the interface. But for  $G > 0.5$ , the chains overlap. For sample 1, the chains are always mutually interacting, leading to a weak (strong) stretching for  $G < 0.65$  ( $G > 0.65$ ). If we assume that the chains are always in the brush regime,<sup>3,16</sup> then the thickness of the interface  $h$  follows the well-known scaling laws:

$$h = aN\sigma^{1/3} \quad \text{in good solvent}$$

$$h = a'N\sigma \quad \text{in poor solvent}$$

$N$  is the polymerization index of the chains,  $\sigma$  is the grafting density, and  $a$  and  $a'$  are typical monomer sizes. We have reported the variation of  $\Delta h/N = 1/N(h(\text{good solvent}) - h(\text{poor solvent}))$  as a function of  $\sigma$  in Figure 13, assuming that  $a \approx a' \approx 1$ .  $\Delta h/N$  is always an increasing function of  $\sigma$ , up to a critical value that is of the order of 0.2, which is huge from an experimental point of view. This simple argument shows that the grafting amplifies the effects of the preferential solvation. They seem however to be qualitatively the same as for dilute polymer solutions in

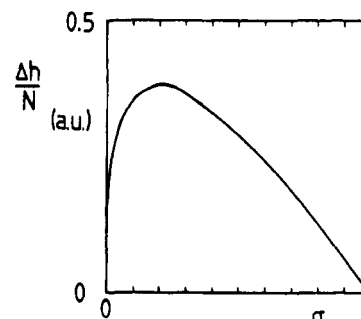


**Figure 13.** Variation of the difference (divided by  $N$ ) between the thickness of a brush in a good solvent and in a poor solvent as a function of the grafting density  $\sigma$ .

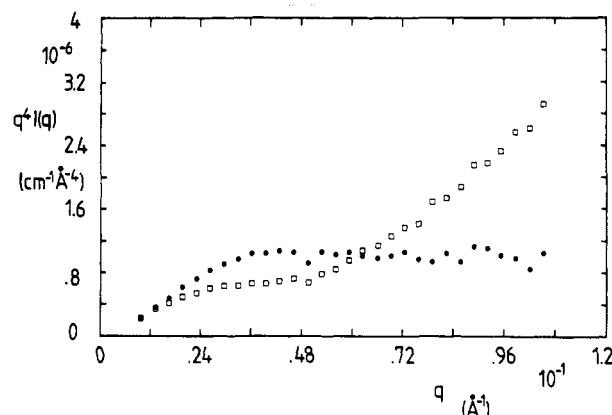


**Figure 14.** Scattering intensity of the polymer interface (sample 2) for  $G = 0.6$  (●) and  $G = 0.7$  (□) (plot of  $q^4 I(q)$  vs  $q$ ).

binary mixtures. The simulations of Madga et al. give a correct description of these effects: namely, the good solvent has the greatest affinity for the polymer and, in a 50/50 binary mixture, the chains contract through this preferential solvation. Undoubtedly, for quantitative predictions, the theory and the calculations should be improved: in particular, they have to take into account the interchain interactions and incorporate the effect of the grafting density.

**III.2. Concentration Fluctuations.** As for sample 1, concentration fluctuations grow when  $G$  becomes close to 1. Again, we have only partial data that are, in addition, of relatively poor accuracy because the scattering intensity is weak.

Nevertheless, we can try to compare these data with those of sample 1. It is especially remarkable that concentration fluctuations appear for sample 2 at  $G \approx 0.7$  (see Figure 14) which corresponds to the point where the  $h$  versus  $G$  curve for sample 1 exhibits an abrupt variation. That means that the collapse-stretching transition occurs at the same chemical composition, independent of the grafting density.

But this transition is however qualitatively very different for both samples. We have reported in Figure 15 the values of  $\xi$  we have determined using a fit with eq 5. In both cases,  $\xi$  is a decreasing function of  $G$ , but the more pronounced this dependence, the weaker the grafting density. Furthermore,  $\xi$  seems to "diverge"<sup>17</sup> at low  $\sigma$  for  $G \approx 0.7$ , whereas at high  $\sigma$ ,  $\xi$  is always finite. This could be reminiscent to the collapse-stretching transition discussed by Halperin<sup>3</sup> (and Zhulina et al.<sup>4</sup>) who suggests that this transition is qualitatively very different depending on the grafting density. The "divergence" of  $\xi$  could be also associated to the fact that the chains are no longer overlapping for  $G < 0.6$ .

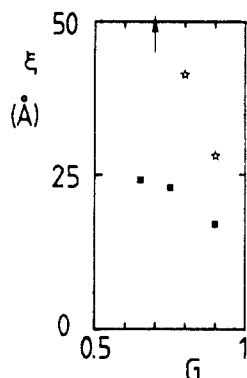


Figure 15. Variation of  $\xi$  as a function of  $G$ : (■) sample 1; (☆) sample 2.

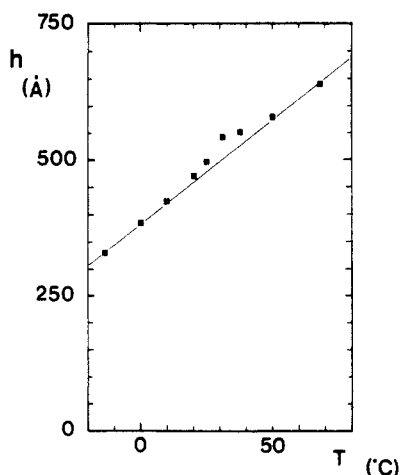


Figure 16. Thickness of the polymer interface (sample 1) as a function of temperature.

**III.3. Applications.** It turns out that grafted PDMS layers are an example of an "environment sensitive system".<sup>18</sup> They open some interesting perspectives from a technological point of view. Obviously, PDMS/silica might not be the most suitable system for many applications. But our study gives a framework for imagining some devices. Indeed, it suggests that at very high grafting density (somewhat higher than that of sample 1), the collapse-stretching transition induced by the preferential solvation would be very steep. One can imagine the use of this feature in some filtration devices that would be very sensitive to the chemical composition of the filtrate.

For instance, above a certain concentration threshold of pollution agent, the membrane (grafted with convenient polymers) would react physically in closing its pores. (The fully stretched chains would greatly reduce the permeability of the membrane.)

One can also imagine to use these grafted chains in separation processes since it turns out that the solvent trapped inside the grafted layers consists of one component, almost pure, of the binary mixture. For that purpose, one should obviously use a substrate with a higher specific surface area.

#### IV. Collapse-Stretching Transition Induced by the Temperature

In this section, we consider only sample 1, immersed in styrene ( $x_D = 52.7\%$ ) at temperature  $T$  ( $-14^\circ\text{C} \leq T \leq 69^\circ\text{C}$ ).

**IV.1. Variation of  $h$  with  $T$ .** In Figure 16, we have reported the variation of the thickness of the interface as a function of temperature.  $h$  increases with  $T$ , but without

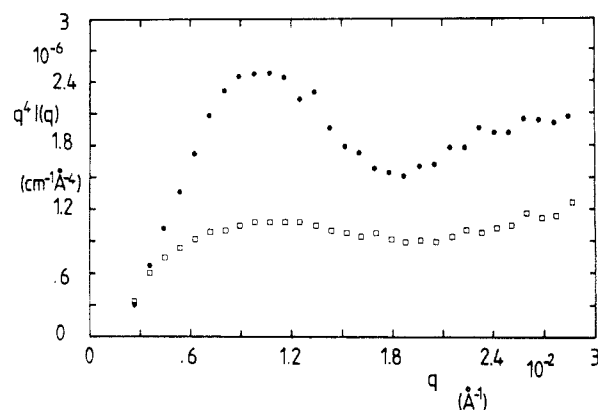


Figure 17. Scattering intensity of the polymer interface (sample 1) for  $T = -14^\circ\text{C}$  (●) and  $T = 70^\circ\text{C}$  (□) (plot of  $q^4 I(q)$  vs  $q$ ).

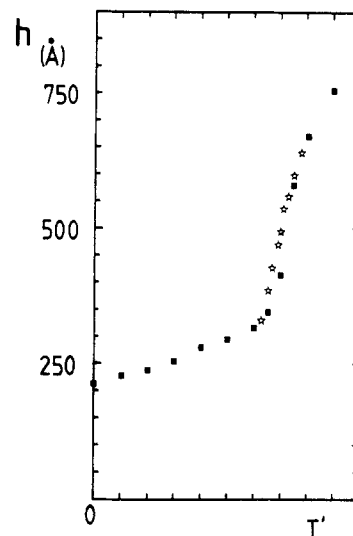


Figure 18. Thickness of the polymer interface (sample 1) as a function of reduced temperature  $T'$ . This reduced temperature has been defined in order to collapse the data of Figures 5 and 16.

any detectable singularities.  $h$  seems to be a linear function of temperature in the whole  $T$  range we have explored.

**IV.2. Shape of the Interfacial Concentration Profile.** The  $q^4 I(q)$  vs  $q$  plots of Figure 17 show that the shape of the interfacial concentration profile gradually changes from a step (oscillations) to a smoother form (with only one well-defined boundary, the solid-polymer border). This is again associated with the growth of concentration fluctuations.

**IV.3. Comparison with the Previous Experiments and with Theory.** All these features are the same as when the collapse-stretching transition is induced by a change of the chemical composition of a binary mixture. But the latter way is much more efficient: a small variation of  $G$  (15%) corresponds to a change of more than 80 deg of temperature. (This is easily seen in Figure 18 where we have collapsed the data of Figures 5 and 16.)

The comparison with theory is not easy because of the systematic use of reduced coefficients. Nevertheless, it was anticipated<sup>4,5</sup> that there should be no phase transition when the temperature is changed provided that the grafting density is high enough. This is in agreement with our observations. The occurrence and the nature of such a phase transition at moderate grafting density is controversial. We cannot give definitive experimental arguments about this point. Indeed, though we have only partial data, we can say that the variation of  $h$  with  $T$  for sample 2 does not exhibit any singularities. But the relative

variation of  $h$  is very weak. Consequently, a kink in this curve is virtually undetectable.

At high grafting density, the theory predicts that  $h$  would scale as  $(T - \theta)^{1/3}$  at high  $T$  (good solvent) and as  $(\theta - T)^{-1}$  at low  $T$  (poor solvent). We find something exactly in between. In the whole  $T$  range we have explored,  $h \approx |T - \theta|$ . Figure 18 suggests that the two asymptotic regimes predicted by the theory have not been attained and the range in which  $T$  has been varied should be enlarged. However, if one makes an expansion around the  $\theta$  temperature of the theoretical expression for  $h$  versus  $T$ , one finds a linear regime<sup>19</sup> that we have indeed observed. We can conclude that our experimental results are at least qualitatively in agreement with the theoretical predictions.<sup>4,5</sup>

## Conclusion

We have shown that the collapse-stretching transition, when it is induced by a change of the chemical composition in a binary mixture, is associated with a strong preferential solvation of the good solvent component. This effect, predicted theoretically for dilute polymer solutions, is much more pronounced for polymer brushes. This could lead to some new filtration or separation processes. When the temperature drives this collapse-stretching transition, the phenomenon is much less spectacular: a large variation of  $T$  is required to change significantly the thickness of the interface.

**Acknowledgment.** We thank A. Lapp for very useful help and G. Jannink for fruitful discussions.

## References and Notes

- (1) Auvray, L.; Cotton, J. P. *Macromolecules* **1987**, *20*, 202. Auvray, L.; Cruz, M.; Auroy, P. Submitted for publication to *J. Phys.*
- (2) (a) Auroy, P.; Auvray, L.; Léger, L. *Phys. Rev. Lett.* **1991**, *66*, 719. (b) Auroy, P.; Auvray, L.; Léger, L. *Macromolecules* **1991**, *24*, 2523. (c) Auroy, P.; Auvray, L.; Léger, L. *Macromolecules* **1991**, *24*, 5158.
- (3) Halperin, A. *J. Phys. Fr.* **1988**, *49*, 547.
- (4) Zhulina, E. B.; Borisov, O. V.; Pryamitsyn, V. A.; Birshtein, T. M. *Macromolecules* **1991**, *24*, 140.

- (5) Brochard, F.; De Gennes, P. G. *Ferroelectrics* **1980**, *30*, 33.
- (6) Magda, J. J.; Frederickson, G. H.; Larson, R. G.; Helfand, E. *Macromolecules* **1988**, *21*, 726.
- (7) Flory, P. *Principles of Polymer Chemistry*; Cornell University Press: Ithaca, NY, 1953. Strazielle, C.; Benoit, H. *J. Phys. Chim.* **1961**, *58*, 678. Cowie, J. M. G. *J. Polym. Sci., Part C* **1968**, *23*, 267. Dondos, A.; Benoit, H. *J. Polym. Sci., Part B* **1969**, *7*, 335.
- (8) Auroy, P.; Auvray, L. *Macromol. Rep.*, in press.
- (9) Lapp, A.; Strazielle, C. *Makromol. Chem., Rapid Commun.* **1985**, *6*, 591. Lapp, A.; Strazielle, C. *Makromol. Chem.* **1985**, *188*, 2921.
- (10) For a complete review of the SANS techniques and the data treatment, see: *Neutron, X-Ray and Light Scattering*; Lindner, P.; Zemb, Th., Eds.; Elsevier Science Publishers BV: Amsterdam, 1991; p 199.
- (11) We have used the following scattering length densities:  $n(\text{CH}_2\text{Cl}_2) = 1.722 \times 10^{10} \text{ cm}^{-2}$ ,  $n(\text{CD}_2\text{Cl}_2) = 3.679 \times 10^{10} \text{ cm}^{-2}$ ,  $n(\text{CH}_3\text{OH}) = -0.337 \times 10^{10} \text{ cm}^{-2}$ ,  $n(\text{CD}_3\text{OD}) = 5.829 \times 10^{10} \text{ cm}^{-2}$ ,  $n(\text{C}_6\text{H}_6) = 1.209 \times 10^{10} \text{ cm}^{-2}$ ,  $n(\text{C}_6\text{D}_6) = 5.521 \times 10^{10} \text{ cm}^{-2}$ ,  $n(\text{P-DMS}) = 0.064 \times 10^{10} \text{ cm}^{-2}$ ,  $n(\text{silica}) = 3.484 \times 10^{10} \text{ cm}^{-2}$ .
- (12) It can be noticed that the absolute normalization of the spectra obtained with the wavelength of 15 Å (Figure 6a) is not the same as that of the two other spectra (obtained with  $\lambda = 6.48$  Å). We can state that the latter spectra are correctly normalized by comparison with the other data. We do not know the origin of this discrepancy. It can be due to multiple scattering, though we have reduced the width of the cell by a factor 2 or to experimental uncertainties. Nevertheless, the ratio  $\beta_1/\beta_2$  is the same for both wavelengths (within a 10% of error). Therefore, our results do not suffer from this discrepancy.
- (13) See ref 12. This value has been obtained with the data corresponding to  $\lambda = 6.48$  Å.
- (14) Hert, M.; Strazielle, C. *Makromol. Chem.* **1974**, *175*, 2149. Aven, R.; Cohen, C. *Makromol. Chem.* **1988**, *189*, 881. Gomez-Anton, M. R.; Masegosa, R. M.; Horta, A. *Makromol. Chem.* **1988**, *189*, 251.
- (15) des Cloiseaux, J.; Jannink, G. *Les Polymères en Solution: leur modélisation et leur structure*; Les Éditions de Physique: Les Ulis, France, 1987.
- (16) Alexander, S. *J. Phys. (Paris)* **1977**, *38*, 983. de Gennes, P. G. *Macromolecules* **1980**, *13*, 1069.
- (17) It was not possible to determine the value of  $\xi$ . The fit of the data with eq 5 gives a negative value for  $\xi^2$  which only indicates that  $\xi$  should be great.
- (18) Hoffman, A. *MRS Bull.* **1991**, Sept, 42.
- (19) Borisov, O.; Zhulina, E. Private communication.

**Registry No.** Methanol, 67-56-1; dichloromethane, 75-09-2; styrene, 100-42-5.